

Electronic Supplementary Information for

Amorphous FeCo oxide as an active and durable bifunctional catalyst for urea-assisted seawater electrolysis

Tianran Wei^{a,b}, Ge Meng^{a*}, Yin Hai Zhou^c, Zhifeng Wang^{d*}, Qian Liu^e, Jun Luo^f, and Xijun Liu^{b*}

a Key Laboratory of Carbon Materials of Zhejiang Province, College of Chemistry and Materials Engineering, Wenzhou University, Wenzhou 325035, China. E-mail: mengge@wzu.edu.cn

b State Key Laboratory of Featured Metal Materials and Life-cycle Safety for Composite Structures, School of Resources, Environment and Materials, Guangxi University, Nanning 530004, China. E-mail: xjliu@gxu.edu.cn

c School of Chemistry & Chemical Engineering, Henan University of Science and Technology, Luoyang 471023, China.

d. School of Materials Science and Engineering, Hebei University of Technology, Tianjin 300401, China. E-mail: wangzjf@hebut.edu.cn

e Institute for Advanced Study, Chengdu University, Chengdu 610106, Sichuan, China.

f ShenSi Lab, Shenzhen Institute for Advanced Study, University of Electronic Science and Technology of China, Longhua District, Shenzhen 518110, China.

Experimental Section

Synthesis

Preparation of *a*-FeCoO, *a*-FeO and *a*-CoO

The catalysts were fabricated by a typical melt-spinning and dealloying method.²⁹ The compositions of the starting materials were designed into Fe_{7.5}Co_{2.5}Al₉₀, Fe₁₀Al₉₀, and Co₁₀Al₉₀ (atomic ratio) ribbons. Firstly, the electric arc melted Fe-Co-Al ingots were remelted in a quartz crucible within a high-frequency induction furnace. After that, the Fe-Co-Al ribbons with different compositions were produced by a single roller melt-spinning technique and were cut into fragments with several centimeters long. Then the as-prepared ribbons (3 g for each experiment) were dealloyed in 500 mL 1 M NaOH solutions at 25 °C for 12 h. During the dealloying process, Al atoms were selectively removed from the alloy, while the remained Fe and Ni atoms were self-oxidized into *a*-FeCoO by combining with OH⁻ and/or oxygen dissolved in the corrosion liquid. After dealloying, the as-obtained products were washed by deionized water for four times to remove the residual Na⁺ species. Then, the samples were heated to 300 °C for 2 h with a ramp rate of 5 °C min⁻¹ under air atmosphere. The synthesis of *a*-FeO and *a*-CoO was similar to the procedure of *a*-FeCoO except for the absence of Co or Fe addition.

Characterization

The morphology and the microstructure of the prepared as-synthesized samples were investigated by SEM (Quanta FEG 250), TEM (Talos F200X), and BET (MIC ASAP2460). The crystalline structures were characterized by Rigaku D/max 2500 X-

ray diffractometer (XRD) with Cu K α radiation ($\lambda = 0.154598$ nm). X-ray photoelectron spectroscopy (XPS, ESCALAB 250Xi, Thermo Scientific) was carried with a monochromatic Al K α radiation source.

UOR and HER tests

The electrochemical measurements were performed using a CHI 760E (CHI Instruments, China) electrochemical workstation at room temperature. A standard three-electrode system was employed for UOR, OER, and HER. The graphite rod and Hg/HgO electrode in saturated KOH were served as the counter electrode and reference electrode, respectively. 5 mg of the samples and 20 μ L Nafion solution were dispersed in 1 mL of ethanol and sonicated for 30 min to form catalyst ink. Subsequently, 10 μ L of the ink was loaded onto the surface of glassy carbon (4 mm in diameter) and dried at room temperature as a working electrode. The seawater from South China Sea (China) was used to prepared electrolyte. The OER and HER measurements were performed in 1.0 M KOH at 5 mV s⁻¹. The UOR performance was tested in 1.0 M KOH + seawater + 0.33 M urea at 5 mV s⁻¹. The recorded potentials were converted into the reversible hydrogen electrode (RHE) according to the Nernst equation.

The cyclic voltammograms (CV) were recorded in 1.0 M KOH + seawater at different scanning rates in the non-faradaic potential region to evaluate the electrochemically active surface area (ECSA) of the catalysts. Electrochemical impedance spectroscopy (EIS) measurements were performed in frequencies from 100 to 0.01 kHz at hydrogen evolution regions.

The Turnover frequency (TOF) value was calculated from the following equation:

$$\text{TOF} = j * A / (6 * F * n)$$

Where j is current density obtained at 1.50 V (vs. RHE) and normalized by geometric area; A is the geometric area; F is the Faraday constant and n is the mole number of active site atoms on the electrode.

Two-electrode measurements

The urea-assisted seawater electrolysis and seawater electrolysis were carried out in a two-electrode configuration using the α -FeCoO as both the cathode and anode in 1.0 M KOH + seawater + 0.33 M and 1.0 M KOH + seawater, respectively. To make the quantitative analysis of the evolved H₂ during the overall seawater splitting, a water drainage method is employed. Firstly, we collected H₂ gas after the electrolysis has been initiated for ~30 minutes when the soluble H₂ gas is saturated in water. Then, we calculated the moles of H₂ generated from cathode with an ideal gas law and the theoretical amount of H₂ evolved by using the Faraday law, respectively.

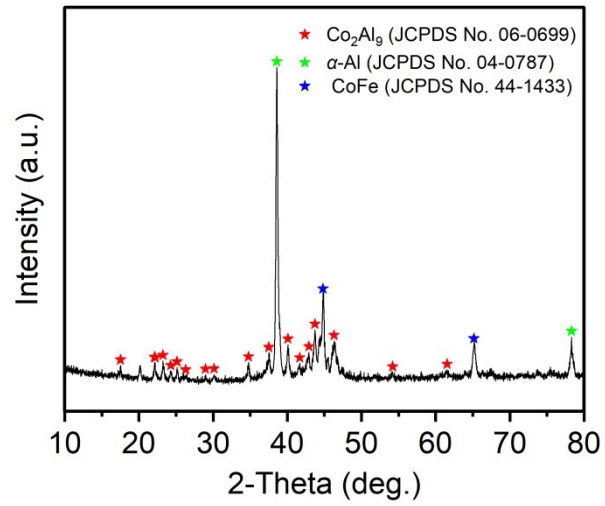


Fig. S1. XRD pattern of the as-prepared $\text{Fe}_{7.5}\text{Co}_{2.5}\text{Al}_{90}$. The peaks can be indexed to Co_2Al_9 , $\alpha\text{-Al}$ and CoFe phases, respectively.



Fig. S2. Photograph of the as-prepared Fe_{7.5}Co_{2.5}Al₉₀.

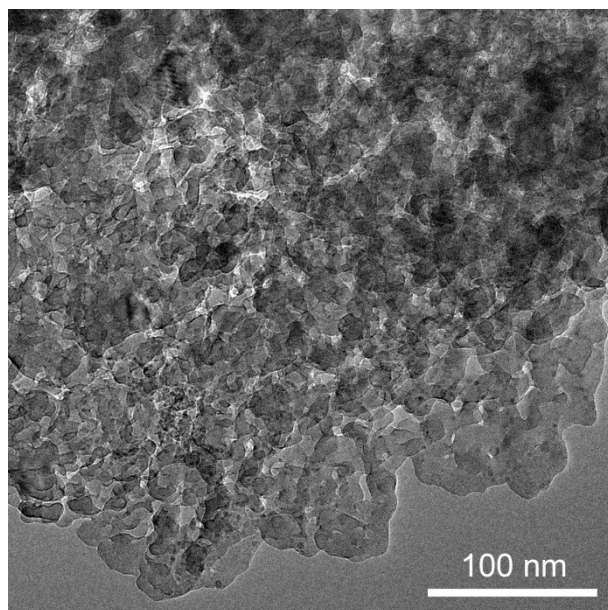


Fig. S3. High-resolution TEM image of the as-synthesized α -FeCoO.

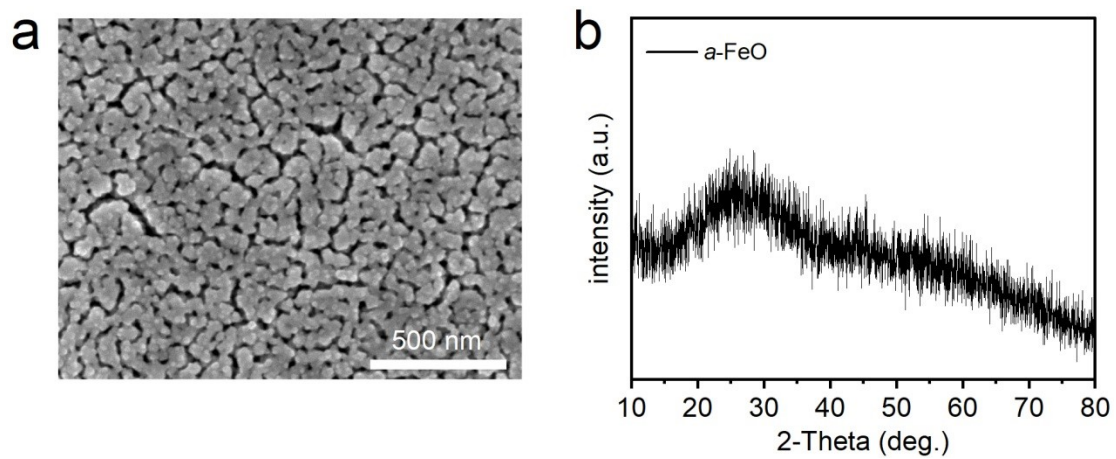


Fig. S4. SEM image and XRD pattern of the as-synthesized α -FeO.

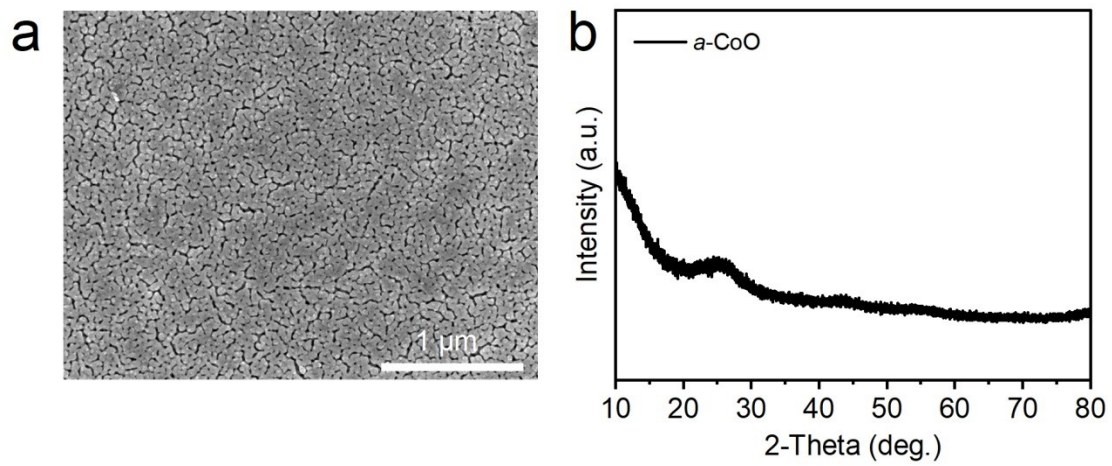


Fig. S5. SEM image and XRD pattern of the as-synthesized α -CoO.

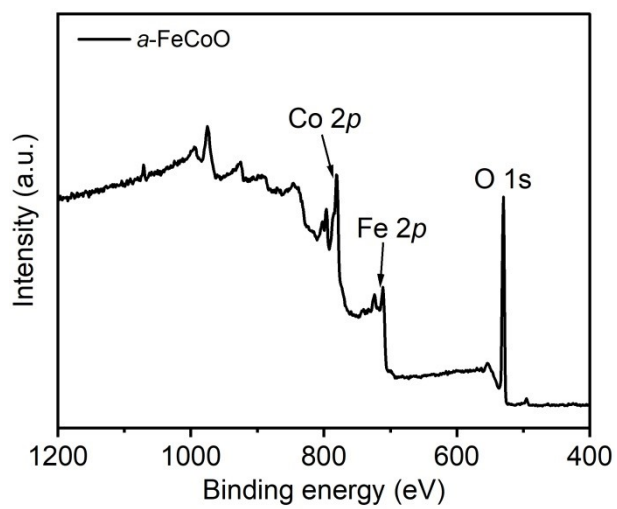


Fig. S6. XPS survey of the as-prepared *a*-FeCoO.

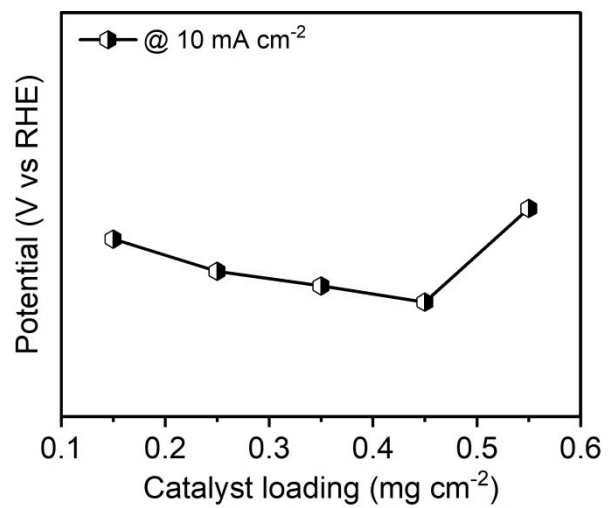


Fig. S7. The effect of α -FeCoO loading on its UOR performance.

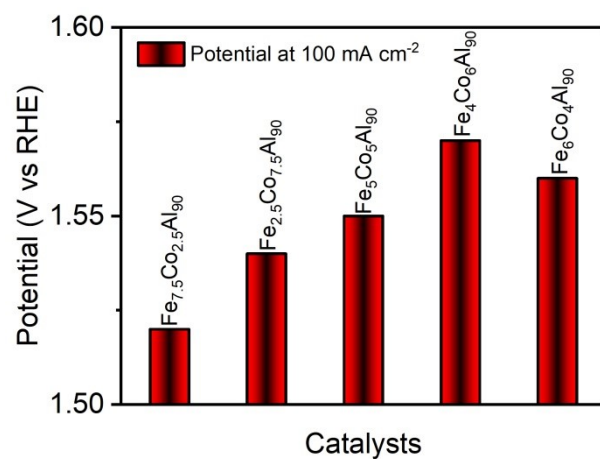


Fig. S8. Potentials at 100 mA cm⁻² for α -FeCoO with different compositions.

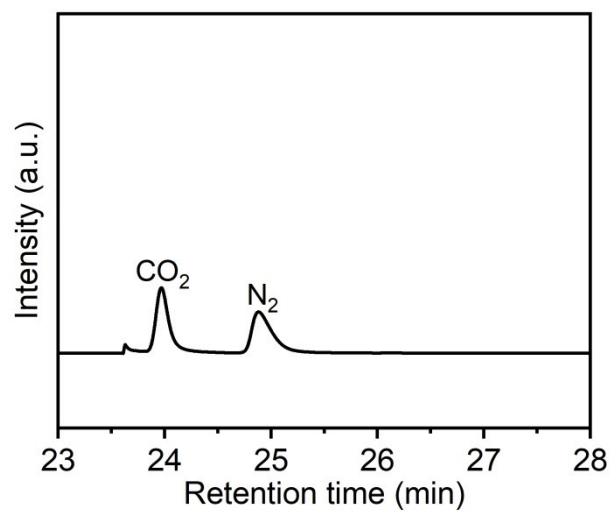


Fig. S9. The produced gaseous products of α -FeCoO during the UOR electrolysis. Clearly, only UOR products (i.e., CO₂ and N₂) are observed and no Cl₂ from the competitive chlorine evolution reaction (CER) is determined.

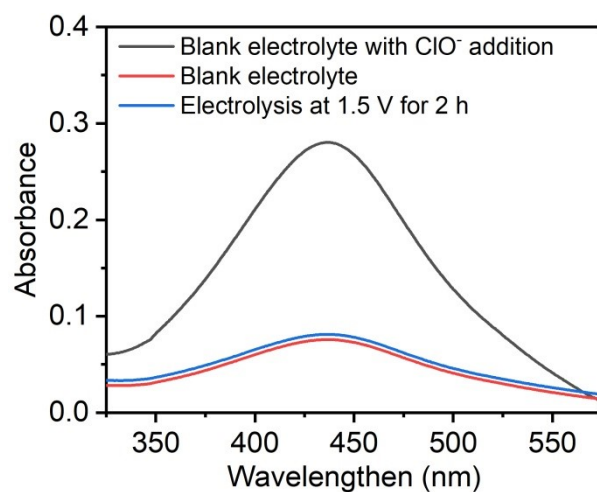


Fig. S10. UV-vis absorption spectra of the electrolytes (0.1 mL) taken from various electrolysis conditions. It is found that no ClO⁻ generation is detected under a potential of 1.5 V vs RHE (*Nature Commun.* 2021, 12, 4182).

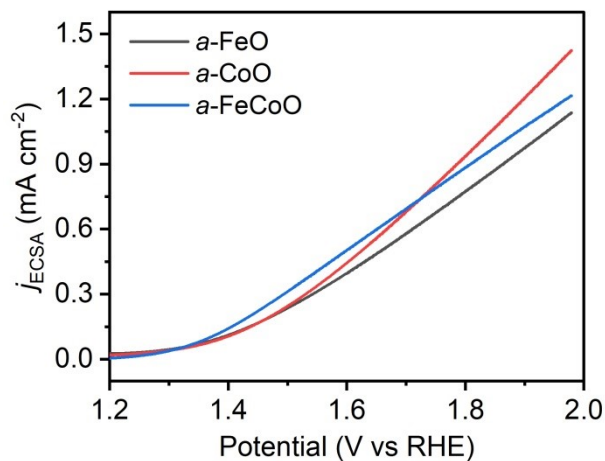


Fig. S11. The ECSA-corrected UOR LSV curves of *a*-FeCoO. As seen, at $j_{\text{ECSA}} = 0.5$ mA cm⁻², *a*-FeCoO needs the lowest potential (1.598 V vs RHE) than those of *a*-FeO (1.659 V vs RHE) and *a*-CoO (1.625 V vs RHE).

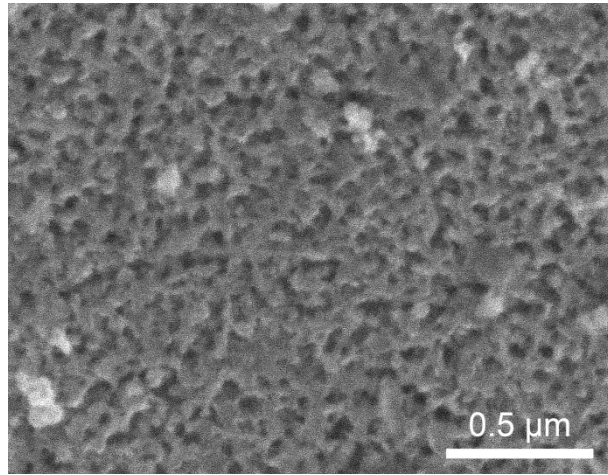


Fig. S12. SEM image of α -FeCoO taken after the UOR electrolysis.

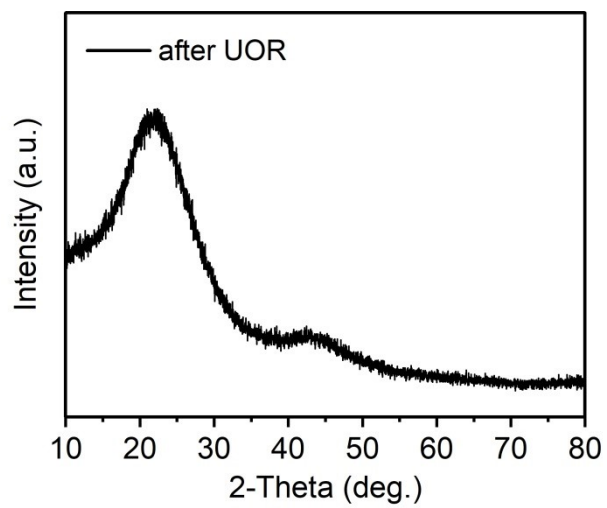


Fig. S13. XRD pattern of α -FeCoO taken after the UOR electrolysis.

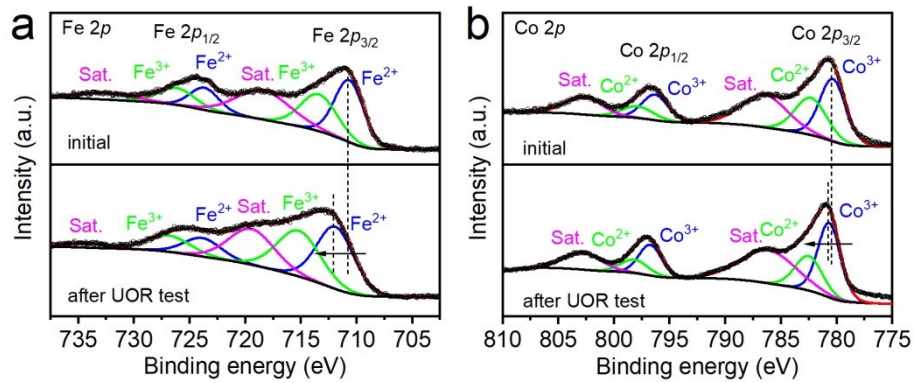


Fig. S14. (a) Fe 2p, (f) Co 2p of *a*-FeCoO before and after the UOR test. From the high-resolution XPS spectra of Fe 2p and Co 2p after the UOR, it is found that more high valence state Fe³⁺ and Co³⁺ species are observed due to the formation of Co(Fe)-(oxy)hydroxides via electro-oxidation (*J. Colloid Interface Sci.* 2023, 645, 724). Besides, it should be noticed that the binding energies of Fe 2p and Co 2p are all positively shifted after the UOR. Previous research has shown that these generated (oxy)hydroxides derived from surface reconstruction are real reactive species, which plays a positive role in catalyst activity and stability for the UOR (*J. Colloid Interface Sci.* 2023, 645, 724; *Int. J. Hydrog. Energy* 2023, 48, 5080).

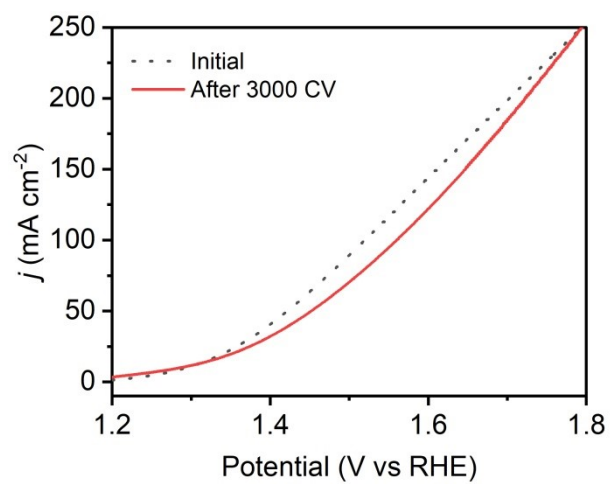


Fig. S15. Cycling stability of α -FeCoO for UOR.

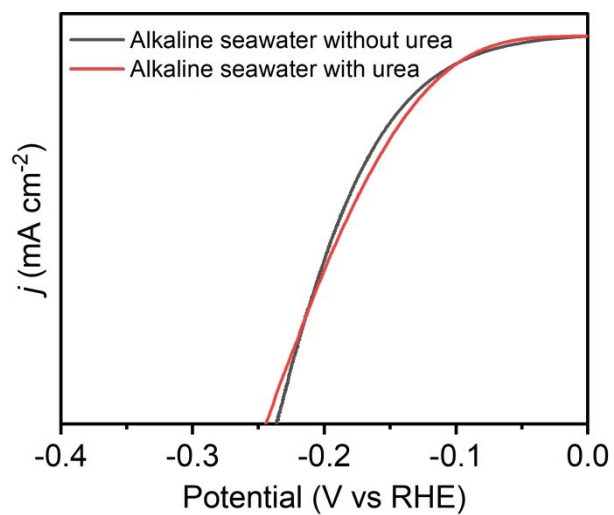


Fig. S16. HER LSV curves of *a*-FeCoO recorded in different electrolytes.

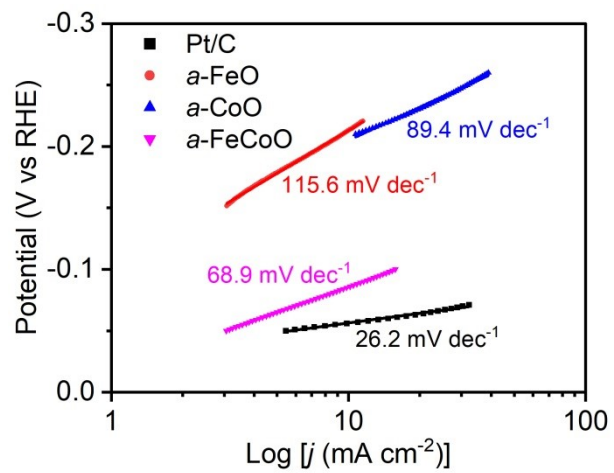


Fig. S17. HER Tafel plots for different samples.

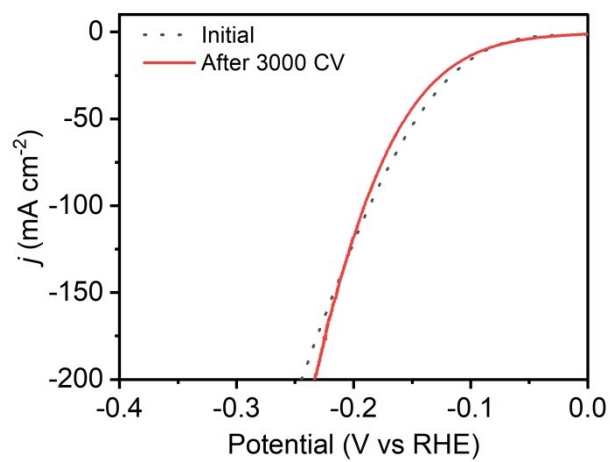


Fig. S18. Cycling stability of α -FeCoO for HER.

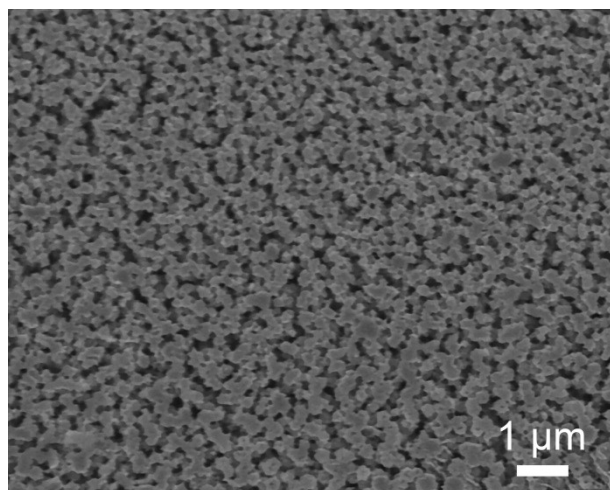


Fig. S19. SEM image of α -FeCoO taken after the HER electrolysis.

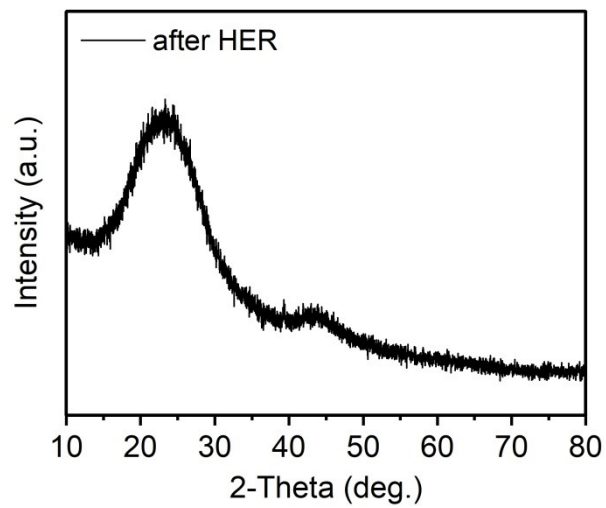


Fig. S20. XRD pattern of α -FeCoO taken after the HER electrolysis.

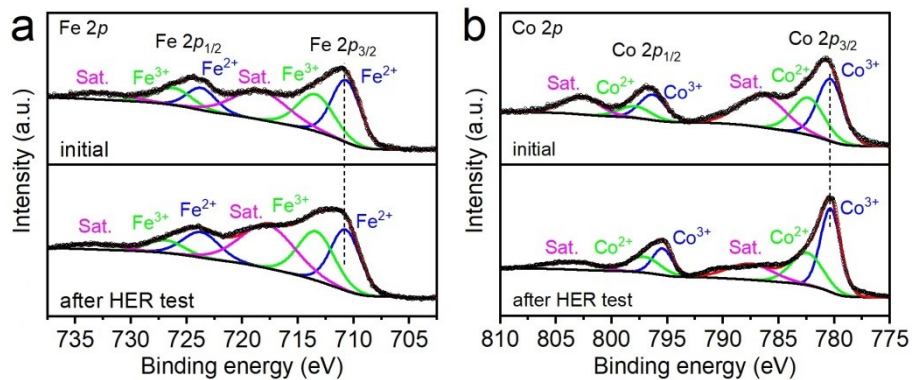


Fig. S21. (a) Fe 2p, (f) Co 2p of *a*-FeCoO before and after the HER test. Analysis of XPS results showed that the characteristic peaks in Fe 2p and Co 2p spectra nearly unchanged after HER stability test, indicating that *a*-FeCoO has good long-term hydrogen evolution durability.

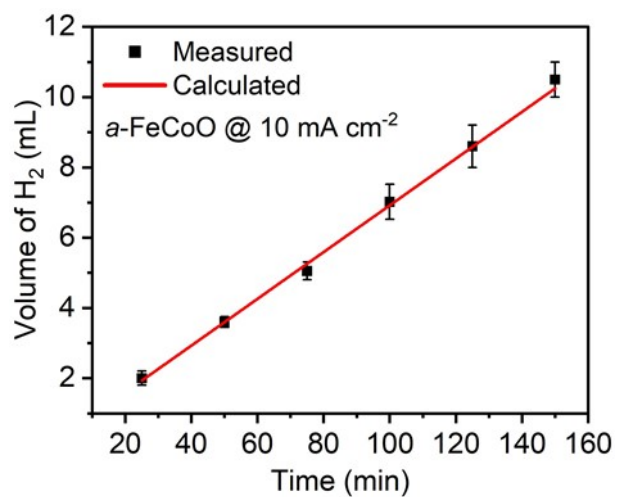


Fig. S22. The evolved H₂ gas amount.

Table S1. The dominated composition of seawater tankan from South China Sea.

Elements	Content (ppm)
Cl⁻	19300
K⁺	300
Na⁺	10800
Ca²⁺	400
Br⁻	70
Mg²⁺	1300
SO₄²⁻	2000

Table S2. Electrocatalysis results from this work and those reported UOR results in the literature.

Catalysts	concentration	E (v)@j (mA cm ⁻²)	Stability	References
(Mn,Ni)O(OH) TSNF	1 M KOH+0.6 M NaCl+0.5M urea	1.35@10 1.40@100	10 h	Surf. Coat. Technol. 408 (2021) 126799.
Se/NiSe ₂ /NF	1 M KOH+ seawater +0.33M urea	1.467@100	20 h	J. Colloid Interface Sci. 630 (2023) 844-854.
Ni ₆₀ Cr ₄₀ /C	1 M KOH+0.33 M urea	1.57@65	NA	ChemCatChem 9 (2017) 3374-3379.
FeCoNiMoRu/CNFs	1 M KOH+0.33 M urea	1.43@100	90 h	Chem. Commun. 59 (2023) 772-775.
Ru/P-NiMoO ₄ @NF	1 M KOH+ seawater +0.5M urea	1.46@1000	24 h	Appl. Catal. B 320 (2023) 121977.
Cu(OH) ₂	1 M KOH+0.5M urea	1.49@10	12 h	Mater. Chem. Phys. 242 (2020) 122517.
Ni-WC/C	1 M KOH+0.33 M urea	1.73@400	NA	Appl. Catal. B 232 (2018) 365-370.
Ni(OH) ₂ -NF	1 M KOH+0.3 M urea	1.61@53	NA	Electrocatalysis 8 (2017) 16-26.
Sn(2)-CoS ₂ /CC	1 M KOH+0.5M urea	1.301@10	108 h	J. Colloid Interface Sci. 642 (2023) 574-583.
CoMn/CoMn ₂ O ₄	1 M KOH+0.5M urea	1.34@20	60000 s	Adv. Funct. Mater. 30 (2020) 2000556.
<i>a</i> -FeCoO	1 M KOH+ seawater +0.5M urea	1.52@100	36 h	This work

Tbale S3. Electrocatalysis results from this work and those reported HER results in the literature.

Catalysts	concentration	η (mv)@j (mA cm ⁻²)	Stability	References
Co/Co ₉ S ₈	1 M KOH + seawater	136.2@10	24 h	Int. J. Hydrogen Energy (2023). https://doi.org/10.1016/j.ijhydene.2023.04.175
CuS	1 M KOH + seawater	199@10	10 h	Int. J. Energy Res. 46 (2022) 19723-19736.
CoSe ₂ -NCF	1 M KOH + seawater	134@10	25 h	Inorg. Chem. Commun. 146 (2022) 110170.
NiFeS/NF	1 M KOH + seawater	347@500	25 h	J. Mater. Chem. A 11 (2023) 1116-1122.
(Co,Fe)PO ₄	1 M KOH + seawater	137@10	72 h	Nanomaterials, 11 (2021) 2989
(Co-Mo-B/NF)	1 M KOH + seawater	199@100	24 h	Molecules, 27 (2022) 7617.
Co-P/NF	1 M KOH + seawater	213@100	50 h	Eur. J. Inorg. Chem. 26 (2023) e202200657.
Ni ₃ N@C/NF	1 M KOH + seawater	142@100	100 h	J. Mater. Chem. A 9 (2021) 13562-13569.
MnCo/NiSe/NF	1 M KOH + seawater	31.4@10	150 h	Appl. Catal. B 325 (2023) 122355.
NiFe-P@NC	1 M KOH + seawater	149@100	12 h	Inorg. Chem. Front. 10 (2023) 1493-1500.
<i>a</i> -FeCoO	1 M KOH+ seawater	86@10 185@100	36 h	This work